Using Vegetation Indices from Hyperspectral Imaging Data to Differentiate Among Invasive Plant Species

Anthony J. Murphy-Neilson
Herndon, Virginia

A Thesis presented to the Faculty
of the University of Virginia
in Fulfillment of the
Distinguished Majors Program

Department of Environmental Sciences

University of Virginia
April 2015

____
Howie Epstein,
Thesis Advisor

____
Thomas A. Smith,
Director of Distinguished Major Program

ABSTRACT

The management of invasive plants is a prevalent area of study and is relevant today in many ecosystems. Vegetation indices from remotely sensed hyperspectral data are useful for identifying invasive plants, as these indices are determined by the different physical and chemical features of plants. Drone-based hyperspectral images collected from a field in northwestern Virginia four individual times during 2020 were used to identify certain invasive plant species. From these images, reflectance spectra were sampled from 15 pixels representative of target individuals and transformed into vegetation indices using the R package hsdar. A partial least squares-discriminatory analysis (PLS-DA) was conducted with the vegetation indices to differentiate individual species and determine indices most useful in differentiation. Two invasive shrub species, autumn olive and Dahurian buckthorn, were each compared to all other plants in the field. The greatest variance explained by components 1 and 2 occurred in November for autumn olive, and June for buckthorn. The components explained a combined 49% of variance for autumn olive in November, and a combined 58% of variance for buckthorn in June. Both species separate particularly strongly across component 1 for both of these months. Buckthorn was particularly well-separated by vegetation indices related to chlorophyll and leaf area index, while autumn olive was most well-separated by vegetation indices related to chlorophyll and stress. However, vegetation indices relating to all physiological factors were useful for both species. Furthermore, buckthorn is particularly differentiable in later months, likely due to it losing its leaves very late. The greatest variance explained by the PLS-DA, paired with the degree of separation among the different plant species, leads me to conclude that June and November are the best times of year to identify autumn olive and buckthorn.

ACKNOWLEDGEMENTS

First, I thank my thesis advisors and mentors in the Department of Environmental Science. I emailed several graduate students on a whim my third year in order to try to get involved in research. Kelsey Huelsman took me under her wing and for the next two years guided me through one of the most valuable academic experiences of my college career. I couldn't have asked for a better mentor. I thank Professor Howie Epstein for being my research advisor, for helping me through the thesis process, helping me eat for free, and helping me imagine what it would be like to take a road trip with David Bowie. I also thank my research partner, Aline Johnson, with whom I learned to navigate R, and presented research with at Envirothon 2021. I also thank my departmental academic advisor, Professor Tom Smith, for helping me navigate college and answering every question I ever asked, even if it meant calling me while in the car with his daughter.

I thank The University of Virginia for making it possible for me to complete this project, and the Department of Environmental Science for making it so easy to get involved in research.

Finally, I thank the Distinguished-Majors-Program committee, led by Professor Thomas Smith, for their feedback and consideration of this project.

TABLE OF CONTENTS

Abstract …………………………………………………………………………………...ii

Acknowledgements……………………………………………………………………iii

Table of Contents ……………………………………………………………………...iv

List of Figures …………………………………………………………………………v

List of Tables …………………………………………………………………………vii

Chapter 1: Introduction…………………………………………………………………1
1.1 Background……………………..…………………………………………………..1
1.2 Rationale ……………..…………………………..………………………….……2
1.3 Objectives ……………..…………………………..………………………….……4

Chapter 2: Methods ……………..………………………..…………………………5
2.1 Study Site & Hyperspectral Data ……………..……………………………..………..5
2.2 Generating vegetation indices from hyperspectral images ……………..…………7
2.3 Differentiating plant species using vegetation indices ……………..………………9
2.4 Variability of vegetation indices over the course of a growing season ……………..9
2.5 Biochemical and phenological characteristics ……………..……………………..10

Chapter 3: Results ……………..………………………..…………………………..10
3.1 Differentiating Autumn Olive ……………..………………………...…………10
3.2 Differentiating Dahurian Buckthorn ……………..…………………………..……12
3.3 Differentiating between times in the growing season ……………..………………14
3.4 Identifying useful vegetation indices ……………..………………………..…...16

Chapter 4: Discussion ……………..………………………..………………………18
4.1 Categorizing Vegetation Indices ……………..………………………..………..18
4.2 Which vegetation indices are most helpful for separation ……………..…………20
4.3 Separating Species by Growing Season……………..…………………………… 26
4.4 Areas for future research ……………..………………………..………………28

Chapter 5: Conclusion ……………..………………………..……………………...29

References ……………..………………………..………………………..……...31

LIST OF FIGURES

Figure 1 Location of field within Blandy Experimental Farm from which hyperspectral data were collected in 2020. Field shown is in early secondary succession…………………………..…….6

Figure 2 PLS-DA for autumn olive (*E. elaeagnus*) vs. all other plants in the field throughout four months. Panel A shows PLS-DA from April (DOY = 106), panel B from June (DOY = 160), panel C from September (DOY = 250), and panel D from November (DOY = 309). In all four analyses, the species of interest separates into the third quadrant of the graph (negative with respect to both components 1 and 2). With 49% of variance explained across components 1 and 2, November is the best month for differentiating this species, but June and September are also very useful, at 46% variance explained. The vegetation indices that load most heavily for either direction of both components can be seen in Table 2……..…11

Figure 3 PLS-DA for Dahurian buckthorn (*R. davurica*) vs. all other plants in the field throughout four months. Panel A shows PLS-DA from April (DOY = 106), panel B from June (DOY = 160), panel C from September (DOY = 250), and panel D from November (DOY = 309). The species of interest separates poorly from the field in April (panel A) and to a lesser extent in September (panel C), and separates in the positive direction with respect to component 1 in June (panel B), and positively with respect to components 1 and 2 in November (panel D). With 58% variance explained across components 1 and 2, June is the best month for differentiating this species. The vegetation indices that load most heavily for either direction of both components can be seen in Table 2……………………13

Figure 4 PLS-DA for autumn olive (*E. elaeagnus*, panel A) and Dahurian buckthorn (*R. davurica*, panel B) comparing the species of interest across four months of study (April, DOY = 106; June, DOY = 160; September, DOY = 250; November, DOY = 309). Panels C and D list the vegetation indices that load heavily in each quadrant for the graph above it (panel C describes PLS-DA in panel A, panel D describes PLS-DA in panel B) based on the quadrants in which those vegetation indices load heavily. For example, Carter 2 loads heavily in the negative direction of component 1 in the PLS-DA for both species. Therefore, it can be found in the lists on the left side of panels C and D, which correspond to heavy loading in the negative x-direction of both graphs. ……………………………………15

Figure 5 This color-coded key applies to tables 3-5 and indicates which VIs are associated with which characteristics. For example, in Table 3, the vegetation index EVI has been printed in blue type, as it is associated with leaf area index (LAI), which is printed in blue type in this figure…………………………………………...………18

LIST OF TABLES

Table 1 Common invasive and non-invasive tree, shrub, forb, and graminoid species that are visible in hyperspectral imagery within the test site. Fifteen spectral samples were taken from well-lit and representative pixels from each individual at four points in the growing season……………………………………………………...8

Table 2 Lists of vegetation indices that correspond most positively and negatively for each species in each PLS-DA for both components. Lists here are shown irrespective of where in the component space the vegetation indices loaded, only whether or not they are positively associated with the species of interest in the component space (as seen in Figures 2 & 3, above). Instances in which the species of interest did not separate significantly in either direction for a given component space are left blank……………..17

Table 3 This table is a recreation of Table in 2 identical in every respect save for the coloring of the various vegetation indices. They are colored in accordance with the key presented in Figure 5, and each color corresponds to a physical parameter measured by or associated with that vegetation index. The purpose of this table is to make is easier to see physical parameter patterns in the vegetation indices presented in Table 2……………………………..…20

Table 4 This is a further simplification of Tables 2 and 3. Instead of listing individual indices, this table lists only the physical parameter categories that make an appearance in Table 3. The purpose of this table is to make it easier to detect patterns in the categories, but it should be noted that no matter how many indices of each category appear in the corresponding cell in Table 3, each category will only be listed once per cell in this table when applicable……………………………………………..22

Table 5 This table is a simplification of Table 4 that erases the distinction between components 1 and 2. The “Positively associated in component 1” and “Positively associated in component 2” columns of Table 4 have been combined into a single column in this table. The same has been done for the “Negatively associated” columns. The purpose of this table is to present the physical categories of the relevant vegetation indices at the simplest level of organization, to allow for easier detection of patterns………………..…24

INTRODUCTION

1.1 *Background*

Globally, invasive plants pose significant threats to natural ecosystems (Gurevitch & Padilla, 2004) and biodiversity (Gaertner et al., 2009; Kimothi & Dasari, 2010; Peerbhay et al., 2016). Across the state of Virginia, invasive, non-native plants are radically altering natural environments by inhibiting the growth of native species upon which native wildlife and insects depend. These widespread changes in species composition also have broader impacts on soil chemistry and vegetation canopies, with effects on dynamics of carbon, nutrients, water, and energy. Invasive plant species monitoring and removal has become an increasingly extensive area of focus in environmental work in recent years, and is relevant and valuable in almost all natural ecosystems. However, there is a lack of capacity to identify invasive species across broad extents of land. The goal of my research is to determine whether filtering hyperspectral data taken by drones through vegetation indices is a reliable method for identifying invasive plant species found in Virginia, and determining what time of year is the best to perform this analysis. Although there are many invasive species of interest in Virginia with negative effects on native populations, I have chosen to focus my research on autumn olive (*Elaeagnus umbellata*) and Dahurian buckthorn (*Rhamnus davurica*) due to their prevalence and relative abundance. They are also representative of many of the factors that contribute to the harmfulness of invasive plant species, such as outcompeting native plants in nutrient-poor environments (Malinich et al., 2017), and changing factors such as soil moisture (Heneghan et al., 2006) and decomposition rates (Heneghan et al., 2006; Mascaro & Schnitzer, 2007).

1.2 *Rationale*

Monitoring Invasive Plants

Controlling the spread of invasive plant species demands extensive ecosystem monitoring. Unmanned aerial vehicles (UAVs, or drones) overcome the spatial and temporal limitations of traditional ground-based and satellite-based approaches and are therefore becoming an increasingly popular method of ecosystem observation, including invasive plant species monitoring. In addition to improvements in spatial and temporal resolution made by UAVs, hyperspectral imaging, which provides detailed spectral information using a large number of narrow, contiguous bands (Chance et al., 2016; Kaufmann et al., 2008), is becoming more common.

Identifying Plants Using Hyperspectral Imaging and Vegetation Indices

Spectral reflectance signatures from hyperspectral imaging are influenced by differences in biophysical and biochemical characteristics of plants (Matongera et al., 2016; Wang et al., 2019; Yang et al., 2016), including: pigments (Mahlein et al., 2010; Xiao et al., 2014), such as chlorophyll (Asner & Martin, 2008; Chance et al., 2016; Thenkabail et al., 2014), anthocyanins, and carotenoids (Blackburn, 2007); plant water and vegetation stress (Thenkabail et al., 2014); and leaf N, P, and K (Asner & Martin, 2008; Chance et al., 2016; Mutanga et al., 2004; Thenkabail et al., 2014). Because UAV flights can take place readily at multiple times during the year, phenological differences in these features among species can aid in differentiation (Castro-Esau et al., 2006).

Thus, hyperspectral data, which serve as an indication of plant chemical and structural properties, vary within and across ecosystems (Martin & Aber, 1997; Ustin et al., 2004). With current understanding of plant chemical and structural properties, hyperspectral data can be used not only to detect general assemblages of plants (Hochberg et al., 2015; Sanchez-Azofeifa et al., 2013; Schmidt & Skidmore, 2003) but also to differentiate among species (Clark et al., 2005; Cochrane, 2000). Imaging spectroscopy is currently the most used approach for studies of invasive plant species (Huang & Asner, 2009) and has been used to identify invasive plant species with both airborne (Aneece & Epstein, 2015; Asner & Martin, 2008; Asner & Vitousek, 2005; Castro et al., 2004; Chance et al., 2016; Kganyago et al., 2017; Skowronek et al., 2017) and handheld (Aneece & Epstein, 2015; Castro et al., 2004; Kganyago et al., 2017) spectrometers.

Though the benefits of analyzing hyperspectral imagery in classification of plant communities are clear, the "big data" provided by hyperspectral imagery can be computationally demanding. Vegetation indices, which are a combination of just a few bands, may be an approach to dimensionality reduction, especially as they can minimize spectral variability caused by solar radiation and viewing angles (Royimani et al., 2019). Wilfong et al. (2009) successfully utilized six vegetation indices in conjunction with Landsat TM satellite imagery to predict *Lonicera maackii* (Amur honeysuckle) invasion in the Midwestern U.S. Using hyperspectral AVIRIS images, Underwood et al. (2007) compared different spatial and spectral resolution combinations to map three invasive species in coastal California. Their most accurate results were derived from images with high spectral resolution. The benefits of high spectral resolution are also supported by Ustin and Jacquemoud's (2020) conclusion that hyperspectral data best capture the subtle responses of reflectance to plant chemical and structural characteristics, which often have overlapping regions within spectra.

Differentiating E. umbellata and R. davurica from other plant species

This study examines two invasive shrub species, *Rhamnus davurica* (Dahurian buckthorn) and *Elaeagnus umbellata* (autumn olive). *R. davurica* is a prevalent invasive shrub in northwestern Virginia. It strongly impacts soil chemistry in communities where it is found, increasing nutrient cycling rates (Mascaro & Schnitzer, 2007); increasing soil C, N, Ca, K, and Mg (Heneghan et al., 2006; Knight et al., 2007); increasing soil moisture (Heneghan et al., 2006); and increasing litter decomposition rates (Heneghan et al., 2006; Mascaro & Schnitzer, 2007). *E. umbellata* is a common invasive shrub; as of 2017 it was found on 39,000 ha in the U.S. (Oliphant et al., 2017). Autumn olive has a relationship with N-fixing endosymbionts and affects nitrifying (ammonium-oxidizing) microorganisms (Malinich et al., 2017; Naumann et al., 2010), and therefore is especially competitive in disturbed areas with N-poor soils (Malinich et al., 2017). In addition to its tolerance of nutrient-poor conditions, *E. umbellata* is also drought resistant and able to survive in a wide range of soil moisture conditions (Malinich et al., 2017; Naumann et al., 2010). Last, it can outcompete native plants after establishment due to its dense shading (Oliphant et al., 2017), a physical property it shares with Dahurian buckthorn.

1.3 *Objectives*

Inspired by the gaps in understanding that might be addressed with UAV-based hyperspectral imaging to differentiate species, my research aims to answer the following questions:

1.) What vegetation indices capture the most spectral variability between *E. umbellata* and other species in the field, to allow for differentiation? How about for *R. davurica*?
2.) When in the growing season are spectra within each species most differentiable using vegetation indices?
3.) What biochemical and phenological characteristics of these species drive the differences in spectral signatures?

By investigating these questions, I will endeavor to work towards a methodology that maximizes efficiency and accuracy for detecting invasive species in Virginia. Creating the final methodology itself is beyond the scope of this project, but I will strive to discover the plant characteristics and vegetation index information necessary to begin such a process. Hopefully, this research will be helpful to scientists working on the same issue and with the means to begin formulating a model to identify invasive species from hyperspectral imagery based on vegetation index data.

METHODS

2.1 *Study Site & Hyperspectral Data Collection*

Blandy Experimental Farm (BEF), a biological field station owned by the University of Virginia, is located in the Shenandoah Valley in northwestern Virginia (39.06ºN, 79.07ºW). At 190 m elevation, BEF has a mean annual precipitation of 975 mm, a mean annual temperature of 12 °C and a mean July maximum temperature of 31.5 °C. It contains 80 ha of old fields in various stages of succession (Bowers, 1997).

Figure 1. Location of field within Blandy Experimental Farm from which hyperspectral data were collected in 2020. Field shown is in early secondary succession.

Aerial hyperspectral data collection took place over a 1-ha field at BEF in early secondary succession (previously subject to disturbance via agriculture), approximately 20 years in age (Figure 1). The field contains abundant invasive shrubs, including *E. umbellata* and *R. davurica* within a heterogeneous matrix of forbs, graminoids, shrubs, and trees.

Spectroscopic images were collected using a DJI Matrice 600 drone equipped with a high-precision GPS system and an imaging spectrometer (Nano-Hyperspec, Headwall Photonics, Bolton, MA). The imaging spectrometer has a spectral range of 400 to 1000 nm (in the visible and NIR portions of the electromagnetic spectrum), with a spectral resolution of 2 to 3 nm over 270 spectral bands. Flight plans over the field were created using Universal Ground Control Software (UgCS), in which the UAV would fly in straight lines at a consistent height of 48 m above the ground in order to obtain images with 3 cm pixels. The entire area of the field could not be captured at this resolution in one image, so multiple images were taken and later pieced together to form a larger image. The imaging spectrometer was programmed to capture images along the flight plan using HyperSpec III software (Headwall Photonics, Bolton, MA). Images were collected at multiple points during the growing season at midday between 10h and 15h in order to reduce bidirectional reflectance distribution function (BRDF) effects and maintain consistent sky conditions. In order to capture seasonal variability and phenological characteristics, images were collected at four times throughout 2020: April 15, June 8, September 6, and November 4 (DOY 106, 160, 250, and 309 respectively) to include early season leaf-out and fall senescence conditions.

Collected spectroscopic images were adjusted for incoming and scattered solar radiation using a sampled dark reference at the time of flight and a white reference tarp located in the flight scene. Using HyperSpec III software, terrain and perspective effects were removed with a digital elevation model provided by the US Geological Survey, and a mosaic of multiple images was created.

2.2 *Generating vegetation indices from hyperspectral images*

In order to answer the questions posed in the Introduction, spectral signatures were collected from 3-cm resolution hyperspectral images for a variety of tree, shrub, and forb species present in a neighboring field, also at Blandy Experimental Farm, used to develop detection algorithms, including *Ailanthus altissima* (tree of heaven), *Rhamnus davurica* (Dahurian buckthorn), *Elaeagnus umbellata* (autumn olive), *Gleditsia triacanthos* (honey locust), *Maclura pomifera* (osage orange), *Juniperus virginiana* (eastern red cedar), *Pinus virginiana* (Virginia pine), *Symphoricarpos orbiculatus* (coralberry), *Galium verum* (yellow bedstraw), *Rubus spp.* (raspberry species), *Catalpa bignonioides* (catalpa), and *Phytolacca americana* (pokeweed). (Table 1) Individuals were identified in the field using a high-precision GPS. Fifteen well-lit and representative pixels were selected for spectral sampling from each individual in images from each collection date.

Table 1. Common invasive and non-invasive tree, shrub, forb, and graminoid species that are visible in hyperspectral imagery within the test site. Fifteen spectral samples were taken from well-lit and representative pixels from each individual at four points in the growing season.

	Plant species	**Growth form**	**Number of Individuals**
Non-native / Invasive	*Elaeagnus umbellata*	Shrub	10
	Rhamnus davurica	Shrub	23
	Ailanthus altissima	Tree	2
	Galium verum	Vine	2
Native / Naturalized	*Gleditsia triacanthos*	Tree	9
	Maclura pomifera	Tree	9
	Prunus virginiana	Tree	2
	Rubus sp.	Shrub	1
	Catalpa bignonioides	Tree	1
	Phytolacca americana	Shrub	1
	Symphoricarpos orbiculatus	Shrub	2
	Juniperus virginiana	Tree	3

Vegetation indices were calculated from extracted spectra using the hsdar package in R (Lehnert et al., 2019). The hsdar package is specifically designed to analyze spectroscopic datasets collected under field conditions with a focus on vegetation and ecosystem applications (Dechant et al., 2017; Große-Stoltenberg et al., 2018; Lehnert et al., 2014; Meyer et al., 2017). Any vegetation indices based on bands beyond 1000 nm were excluded, as the range of the HyperSpec imager does not extend beyond that wavelength.

2.3 *Differentiating plant species using vegetation indices*

Using the dataset generated via hsdar, the spectral signatures were then analyzed using a partial least squares discriminatory analysis (PLS-DA; Barker & Rayens, 2003), which classifies individuals into different groups using the values of the vegetation indices. The data was recoded into each species of interest compared to all other species (i.e., *E. umbellata* compared to all other species; and *R. davurica* compared to all other species). In order to determine when in the growing season differentiating features of *E. umbellata* and *R. davurica* are most detectable via UAV, a separate PLS-DA was performed for each date in the growing season (DOY 106, 160, 250, and 309) with species as the variable of interest. The amount of separation between the two categories (species of interest vs. all other species) indicates times in the growing season when each species of interest is particularly detectable. After an initial PLS-DA, outliers were identified and removed from the dataset manually. Following this, loading factors were examined. Loading factors are indicative of the variables (in this case, vegetation indices) that are particularly useful in differentiating individual species of interest from all other species.

2.4 *Variability of vegetation indices over the course of a growing season*

In order to determine how vegetation indices vary within a single species over the course of the growing season, I analyzed the observations of *E. umbellata* and *R. davurica* individually. I used PLS-DA to classify observations into different groups using DOY rather than species as the separating variable. Following the PLS-DA, loading factors were examined, which indicate which vegetation indices vary most over the course of the growing season.

2.5 *Biochemical and phenological characteristics*

The hsdar documentation includes references for the vegetation indices calculated. I referred to the original work by each author to determine the biochemical relevance of each vegetation index. Pairing this information with vegetation indices that load heavily, and where observations are in the PLS-DA component space, can provide information about which characteristics allow for separation among species throughout the growing season and phenological characteristics of these individual species of interest throughout the growing season.

RESULTS

3.1 *Differentiating Autumn Olive*

Autumn olive differentiated significantly in all months, but in some more strongly than others. An examination of Figure 2 reveals that the species of interest (*Elaeagnus umbellata*) separated into the negative component space in both component one and component two for all four months, relative to both the zero point and to the other species. This places autumn olive in the third quadrant of each graph, but to differing degrees. Furthermore, the species of interest separates more clearly along component 1 than component 2, and has less area of overlap in that direction, but interestingly the PLS-DA reveals that in all cases, component 2 explains more variance than component 1.

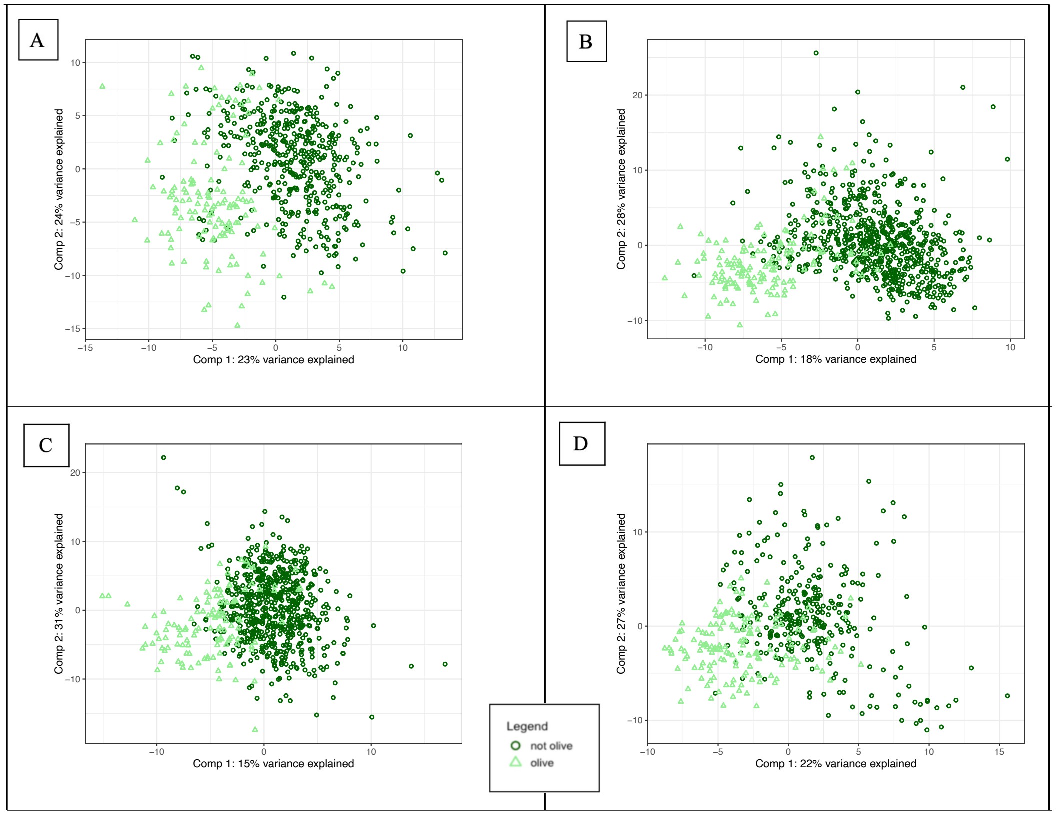

Figure 2. PLS-DA for autumn olive (*E. elaeagnus*) vs. all other plants in the field throughout four months. Panel A shows PLS-DA from April (DOY = 106), panel B from June (DOY = 160), panel C from September (DOY = 250), and panel D from November (DOY = 309). In all four analyses, the species of interest separates into the third quadrant of the graph (negative with respect to both components 1 and 2). With 49% of variance explained across components 1 and 2, November is the best month for differentiating this species, but June and September are also very useful, at 46% variance explained. The vegetation indices that load most heavily for either direction of both components can be seen in Table 2.

In April (DOY 106, panel A in Figure 2), component 1 explains 23% of variance, and component 2 explains 24% of variance. In June (DOY 160, panel B in Figure 2), component 1 explains 18% of variance, and component 2 explains 28% of variance. In September (DOY 250, panel C in Figure 2), component 1 explains 15% of variance, and component 2 explains 31% of variance. Finally, in November (DOY 309, panel D in Figure 2), component 1 explains 22% of variance, and component 2 explains 27% of variance.

Although the most variance is explained in component 2 of the data from September, that is one of the months with the greatest degree over overlap between the target species and the rest of the field, and the data does not separate strongly in any direction along that axis. The most significant separation of the species of interest from the rest of the field occurs in component 1 of the data from June, and to a slightly lesser extent component 1 of the data from September and November. The data from April are also useful for separating out this species of interest, as it shows a relatively small degree of overlap with the non-target species, and has the second-highest variance explained at 47%.

3.2 *Differentiating Dahurian Buckthorn*

Unlike autumn olive, Dahurian buckthorn (*Rhamnus davurica*) separated clearly from the rest of the field in fewer than all four months. An examination of Figure 3 reveals that this species tended towards the positive direction in component 1 in all cases, but for two of the months (April and June, panels A and B in Figure 3), there is no clear differentiation in any direction in component two. However, for September and November (panels C and D in Figure 3), it separates out in the positive direction, the opposite of what autumn olive did. For all months, buckthorn separates along component 1 in the positive direction compared to the rest of the field, but any separation in the component two direction is only present in September and November, and not particularly strong. Furthermore, the separation of the species of interest in April (DOY 106, panel A in Figure 3) is so weak as to almost be negligible. The only apparent separation is a slight tendency to the positive direction in component one.

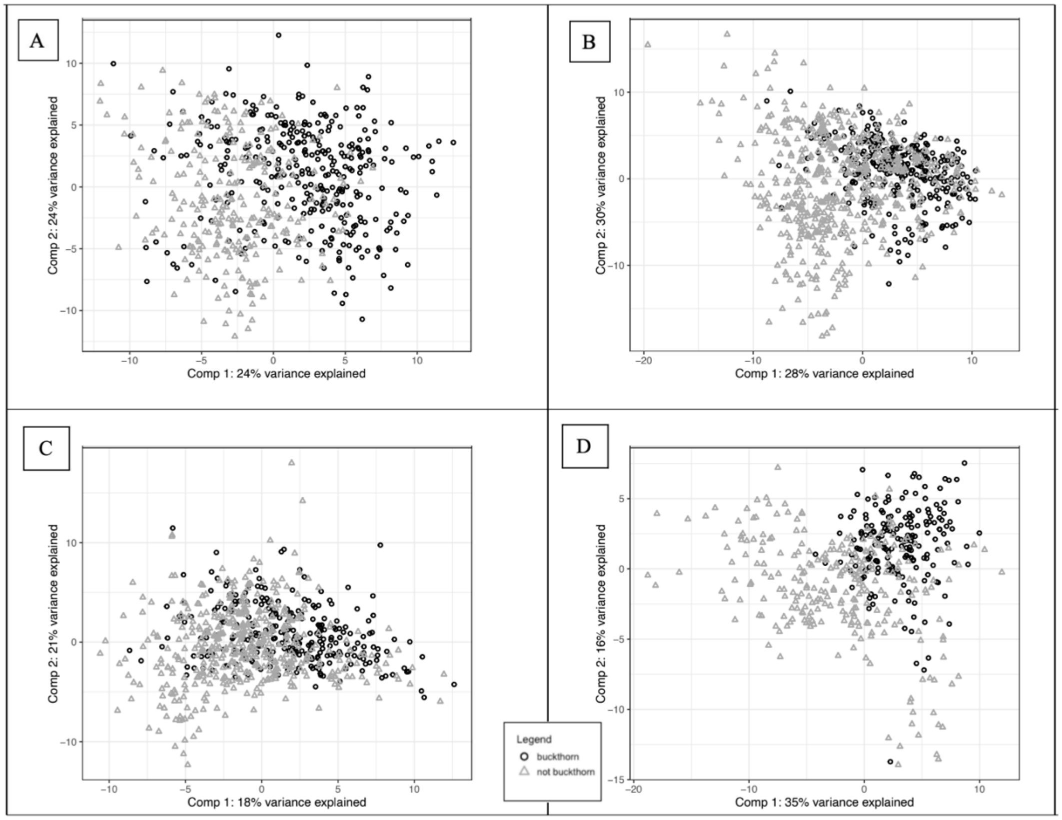

Figure 3. PLS-DA for Dahurian buckthorn (*R. davurica*) vs. all other plants in the field throughout four months. Panel A shows PLS-DA from April (DOY = 106), panel B from June (DOY = 160), panel C from September (DOY = 250), and panel D from November (DOY = 309). The species of interest separates poorly from the field in April (panel A) and to a lesser extent in September (panel C), and separates in the positive direction with respect to component 1 in June (panel B), and positively with respect to components 1 and 2 in November (panel D). With 58% variance explained across components 1 and 2, June is the best month for differentiating this species. The vegetation indices that load most heavily for either direction of both components can be seen in Table 2.

In April (DOY 106, panel A in Figure 3), component 1 explains 24% of variance, and component 2 explains 24% of variance. In June (DOY 160, panel B in Figure 3), component 1 explains 28% of variance, and component 2 explains 30% of variance. In September (DOY 250, panel C in Figure 3), component 1 explains 18% of variance, and component 2 explains 21% of variance. Finally, in November (DOY 309, panel D in Figure 3), component 1 explains 35% of variance, and component 2 explains 16% of variance.

The most helpful months for differentiating buckthorn from the rest of the field are June and November. June shows a strong differentiation in component 1, and November shows a strong differentiation in both components. The differentiation in component 1 for November is particularly strong, with 35% of the variation being explained, the highest of all the PLS-DAs. Although it is clear that there is a higher density of buckthorn in the positive x-direction for the April data, the separation is poor and this would be the worst month to use for this species. September is better, as buckthorn separates significantly in component 1 and slightly in component 2, but not as strongly as component 1 in June or both components in November.

3.3 *Differentiating between times in the growing season*

A PLS-DA comparing each species of interest against itself across the four different months is visible in Figure 4. The results for autumn olive, in panel A, show an extreme amount of overlap across the four months. The vast majority of the data from April, September, and November overlap with the data from at least one other month. The June data, however, separates out slightly better, and separates itself in the positive direction in component 1 and the negative direction in component 2. It is definitely the most strongly separated out of the four months for this species, but most of its data still overlap with at least one other month. This correlates with the observation in section 3.1 that June appeared to show the strongest separation of the species of interest from the rest of the field for autumn olive. In panel A of Figure 4, 43% of the variance is explained in component 1, and in component 2, 14% of the variance is explained.

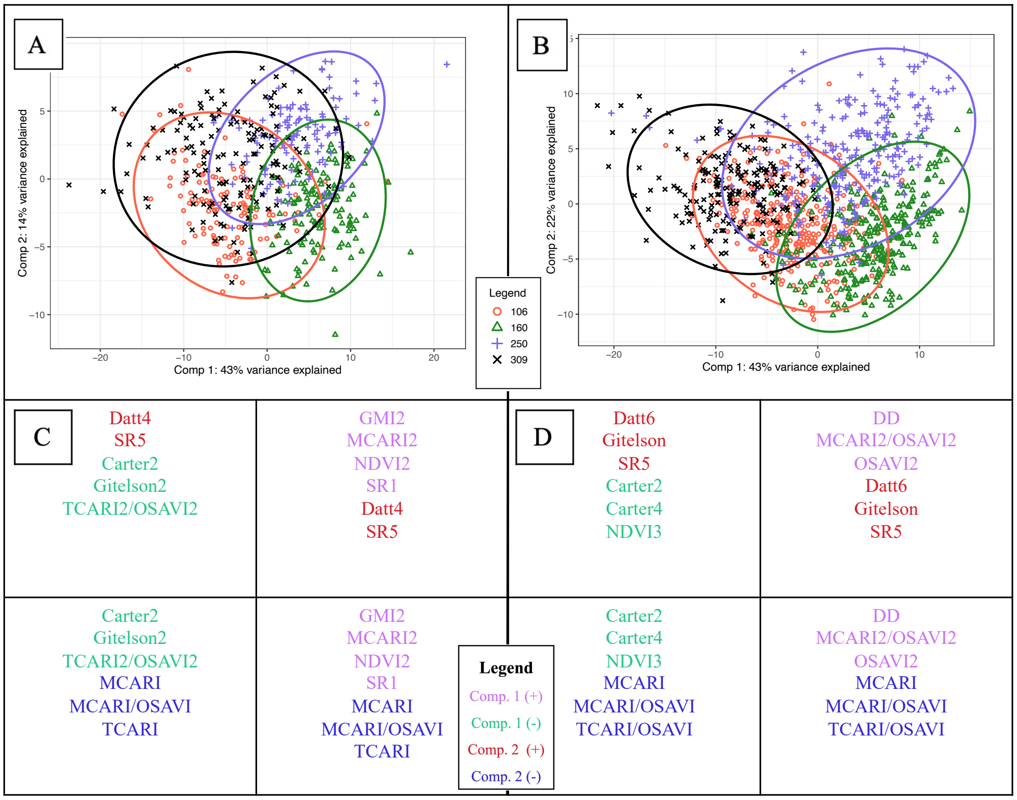

Figure 4. PLS-DA for autumn olive (*E. elaeagnus*, panel A) and Dahurian buckthorn (*R. davurica*, panel B) comparing the species of interest across four months of study (April, DOY = 106; June, DOY = 160; September, DOY = 250; November, DOY = 309). Panels C and D list the vegetation indices that load heavily in each quadrant for the graph above it (panel C describes PLS-DA in panel A, panel D describes PLS-DA in panel B) based on the quadrants in which those vegetation indices load heavily. For example, Carter 2 loads heavily in the negative direction of component 1 in the PLS-DA for both species. Therefore, it can be found in the lists on the left side of panels C and D, which correspond to heavy loading in the negative x-direction of both graphs.

Panel B of Figure 4, showing the PLS-DA across four months for buckthorn, shows much more separation among months. This is not true for all four months; in fact, the April data for buckthorn are the most poorly separated across either species of interest. The June data for buckthorn separate out only modestly, showing significant overlap with the April data and some of the September data, but still roughly about as strongly differentiated as this month was for autumn olive. On the other hand, the September and November data separate very strongly in this graph for buckthorn. Both months show significant portions of their data not overlapping with any of the other months. This is particularly true of September, which appears to have more than 50% of its data almost entirely separated from data from other months. These observations correspond to the observations from section 3.2, which suggested that buckthorn separates out very poorly in April, but much more strongly in other months. Based on the separation apparent in both Figures 3 and 4, it would appear that November is the most useful month for separating buckthorn from other species. For the graph in panel B of Figure 4, 43% of the variance in component 1 is explained, and 22% of the variance in component 2 is explained.

3.4 *Identifying useful vegetation indices*

After running a PLS-DA on each species of interest, both against the rest of the field and against itself across four months, the vegetation indices that contributed most strongly to the PLS-DA were identified. Panels C and D of Figure 4 are each divided into quadrants, showing the vegetation indices that loaded most strongly in those quadrants for the corresponding PLS-DA (panel C corresponds to panel A, panel D to panel B). Since the vegetation indices were used separately in components 1 and 2, they appear to repeat in the four quadrants of the panel. For example, for the PLS-DA of autumn olive across four months (panel A in Figure 4), the vegetation index SR5 loaded heavily in the positive direction of component 2, so it is listed in quadrants I and II of panel C. The vegetation index SR1 loaded heavily in the positive direction of component 1, so it is listed in quadrants I and IV of panel C. For each PLS-DA, the 2-5 vegetation indices that loaded the most heavily, and are therefore most important for the separation of the species of interest, were presented.

Table 2. Lists of vegetation indices that correspond most positively and negatively for each species in each PLS-DA for both components. Lists here are shown irrespective of where in the component space the vegetation indices loaded, only whether or not they are positively associated with the species of interest in the component space (as seen in Figures 2 & 3, above). Instances in which the species of interest did not separate significantly in either direction for a given component space are left blank.

DOY	Species	Positively associated w/ species in component 1	Negatively associated w/ species in component 1	Positively associated w/ species in component 2	Negatively associated w/ species in component 2
106 (Apr.)	*E. umbellata*	EVI, MPRI, R0, SR5	CRI1, PSND, SR4	DD, mSR705, mND705	PSRI, Carter4, Vogelmann4
	R. davurica	DWSI4, GI, MCARI, MCARI/OSAVI	Datt5, NDVI3		
160 (Jun.)	*E. umbellata*	GMI1, mSR2, SR3, SR6	Carter3, Carter4, TCARI2, TCARI2/OSAVI2	TCARI, GI, MCARI, TGI	Datt4, Datt5, NDVI3
	R. davurica	TCARI, TGI, TCARI/OSAVI	Datt4, MTCI, Maccioni		
250 (Sep.)	*E. umbellata*	MPRI, R0, SR5, SR8	DWSI4, GI, SR4	REP_Li, Datt2, MTCI	Vogelmann2, Vogelmann4
	R. davurica	MCARI, GI, MCARI/OSAVI	SR5, PRI, SR8, MTCI	DDn, Gittleson, PRI_norm, PSSR	CIAInt, CARI
309 (Nov.)	*E. umbellata*	Carter6, MPRI, R0, SR5, SR7	DDn, SR4	PRI_norm, SR5	MCARI, SR4
	R. davurica	Vogelmann2, Vogelmann4	DD, MTCI, Maccioni	GDVI_2, GDVI_3, NDVI	PRI_norm, SIPI, SR5

Table 2 shows the vegetation indices that loaded most heavily in each component for the graphs in Figures 2 and 3. As above, the 2-5 vegetation indices that loaded most heavily were presented. However, instead of organizing the table by whether the VIs loaded heavily in either the positive or negative direction of each component space, they were organized according to whether they were correlated positively or negatively with the species of interest in that component. For example, autumn olive separates in the negative direction for both components 1 and 2 for June (panel B of Figure 2), so vegetation indices listed as positively associated with the species of interest in Table 2 are those that loaded most negatively in components 1 and 2 for autumn olive in June.

DISCUSSION

4.1 *Categorizing Vegetation Indices*

Different vegetation indices are useful for indicating different plant characteristics. Most indices relate to the concentration of one or more pigments (e. g. chlorophyll a, chlorophyll b, carotenoids, etc.), but others are helpful for detecting stress levels in plants, are particularly sensitive to the leaf area index (LAI), or focus specifically on the red-edge region of the reflectance spectrum. In attempting to make sense of the data collected from the PLS-DAs, I sorted the relevant vegetation indices (all those that appear in Table 2) by the plant characteristics with which they are most heavily associated.

Figure 5. This color-coded key applies to tables 3-5 and indicates which VIs are associated with which characteristics. For example, in Table 3, the vegetation index EVI has been printed in blue type, as it is associated with leaf area index (LAI), which is printed in blue type in this figure.

Chlorophyll
Leaf Area Index
Stress
Red-Edge
Other

Tables 3 – 5 are all derived from the data presented in Table 2. Table 3 associates vegetation indices with the characteristic they are most useful for observing by highlighting each VI in a color that corresponds to a particular trait (vegetation indices useful for measuring chlorophyll concentration, for example, appear in green). Tables 4 and 5 simplify these results, with Table 4 showing the categories of plant characteristics the vegetation indices measure instead of individual vegetation indices themselves. Table 5 simplifies further by removing the distinction between components 1 and 2 from the PLS-DAs.

Table 3. This table is a recreation of Table in 2 identical in every respect save for the coloring of the various vegetation indices. They are colored in accordance with the key presented in Figure 5, and each color corresponds to a physical parameter measured by or associated with that vegetation index. The purpose of this table is to make is easier to see physical parameter patterns in the vegetation indices presented in Table 2.

DOY	Species	Positively associated in component 1	Negatively associated in component 1	Positively associated in component 2	Negatively associated in component 2
106 (Apr.)	*E. umbellata*	EVI, MPRI, R0, SR5	CRI1, PSND, SR4	DD, mSR705, mND705	PSRI, Carter4, Vogelmann4
	R. davurica	DWSI4, GI, MCARI, MCARI/OSAVI	Datt5, NDVI3		
160 (Jun.)	*E. umbellata*	GMI1, mSR2, SR3, SR6	Carter3, Carter4, TCARI2, TCARI2/OSAVI2	TCARI, GI, MCARI, TGI	Datt4, Datt5, NDVI3
	R. davurica	TCARI, TGI, TCARI/OSAVI	Datt4, MTCI, Maccioni		
250 (Sep.)	*E. umbellata*	MPRI, R0, SR5, SR8	DWSI4, GI, SR4	REP_Li, Datt2, MTCI	Vogelmann2, Vogelmann4
	R. davurica	MCARI, GI, MCARI/OSAVI	SR5, PRI, SR8, MTCI	DDn, Gittleson, PRI_norm, PSSR	CIAInt, CARI
309 (Nov.)	*E. umbellata*	Carter6, MPRI, R0, SR5, SR7	DDn, SR4	PRI_norm, SR5	MCARI, SR4
	R. davurica	Vogelmann2, Vogelmann4	DD, MTCI, Maccioni	GDVI_2, GDVI_3, NDVI	PRI_norm, SIPI, SR5

4.2 *Which vegetation indices are most helpful for separation*

The vegetation indices most useful for separating each species of interest are listed in Table 2, and sorted according to the plant characteristic they are most indicative of in Table 3. Several patterns can be observed from these tables. Since most vegetation indices are related to chlorophyll content, it is not surprising that VIs in this category appear ubiquitously across this table. Chlorophyll content is the most direct plant characteristic to measure using this method. It is interesting, however, that indices related to red-edge characteristics are never positively associated with the species of interest in component 1, and are always positively associated with the species of interest in component 2, as seen in Table 4. This may be an indicator that red-edge is not a particularly useful factor in this type of analysis, as most PLS-DAs showed the species of interest separating along component 1 more than component 2. In contrast, LAI-related indices occur much more often when positively associated with the species of interest, and only rarely when negatively associated. This could indicate that LAI-related indices are particularly useful in this type of analysis. The only characteristic evenly distributed across components 1 and 2 is indices related to chlorophyll concentration. It appears in every box of Table 4 but one, and is useful in its broad applicability, but is likely too ubiquitous to be particularly helpful for discrimination or dimensionality reduction of the data set.

Patterns can also be seen by comparing plants instead of components. For example, as seen in Table 3, autumn olive (8 instances) is far more likely than buckthorn (3 instances) to have a strong association, positive or negative, with vegetation indices related to stress. It would follow from this observation that autumn olive exhibits stress in a way that makes it visibly different from other plants, while perhaps buckthorn exhibits stress in a similar way to other plants, making it less of a distinguishing factor from the rest of the field. Furthermore, autumn olive is strongly separated by indices associated with LAI mostly in the earlier months. In June in particular, LAI-related indices appear very often. June is the most useful month for separating olive from the rest of the field, so it seems LAI-focused indices at this time of year would be the most effective way to differentiate autumn olive from a field. This is in contrast to buckthorn, which has LAI-related indices occurring evenly throughout the four months. This may not be the most useful category of VIs for differentiating buckthorn.

Table 4. This is a further simplification of Tables 2 and 3. Instead of listing individual indices, this table lists only the physical parameter categories that make an appearance in Table 3. The purpose of this table is to make it easier to detect patterns in the categories, but it should be noted that no matter how many indices of each category appear in the corresponding cell in Table 3, each category will only be listed once per cell in this table when applicable.

DOY	Species	Positively associated in component 1	Negatively associated in component 1	Positively associated in component 2	Negatively associated in component 2
106 (Apr.)	*E. umbellata*	Chlorophyll LAI Stress Other	Chlorophyll Other	Chlorophyll Red-edge	Chlorophyll Stress Other
	R. davurica	Chlorophyll Stress	Chlorophyll LAI		
160 (Jun.)	*E. umbellata*	Chlorophyll LAI	Chlorophyll Stress	Chlorophyll LAI	Chlorophyll LAI
	R. davurica	Chlorophyll LAI	Chlorophyll Red-edge		
250 (Sep.)	*E. umbellata*	Chlorophyll Stress Other	Chlorophyll Stress	Chlorophyll LAI Other	Chlorophyll
	R. davurica	Chlorophyll	Chlorophyll Red-edge	Chlorophyll Red-edge	Chlorophyll
309 (Nov.)	*E. umbellata*	Chlorophyll Stress Other	Chlorophyll Red-edge	Chlorophyll	Chlorophyll
	R. davurica	Chlorophyll	Chlorophyll Red-edge	LAI Stress	Chlorophyll Stress

Perhaps the strongest pattern of all can be extracted from Table 3, looking at the autumn olive data for April, September, and November. For all three of these months, three vegetation indices in particular are strongly correlated with the species of interest in component 1. One is a red-edge associated index that measures reflectance at the red-edge minimum (R0), one is a chlorophyll-related index that estimates the concentration of chlorophylls a and b by gathering reflectance at 675 and 700 nm (SR5), and one is a stress-related index that measures reflectance at 515 and 530 nm (MPRI). In all the data, this is the only time any individual indices show up consistently correlated with the same plant in the same way. This would indicate that these three indices are extremely useful for identifying autumn olive at most times of year. The only break from this pattern is June, which is also when autumn olive shows the strongest separation from the field in Figure 2. However, the separation is still present in the other months, and can be useful for differentiating this plant. These results would indicate that autumn olive behaves in a particularly different way from other plants in June (likely related to chlorophyll content and LAI, as seen in Table 4). But for the rest of the year, its innate differences from other plants are particularly noticeable with the vegetation indices MPRI, R0, and SR5.

Table 5. This table is a simplification of Table 4 that erases the distinction between components 1 and 2. The "Positively associated in component 1" and "Positively associated in component 2" columns of Table 4 have been combined into a single column in this table. The same has been done for the "Negatively associated" columns. The purpose of this table is to present the physical categories of the relevant vegetation indices at the simplest level of organization, to allow for easier detection of patterns.

DOY	Species	Positively associated	Negatively associated
106 (Apr.)	*E. elaeagnus*	Chlorophyll LAI Stress Red-edge Other	Chlorophyll Stress Other
	R. davurica	Chlorophyll Stress	Chlorophyll LAI
160 (Jun.)	*E. elaeagnus*	Chlorophyll LAI	Chlorophyll Stress LAI
	R. davurica	Chlorophyll LAI	Chlorophyll Red-edge
250 (Sep.)	*E. elaeagnus*	Chlorophyll Stress LAI Other	Chlorophyll Stress
	R. davurica	Chlorophyll Red-edge	Chlorophyll Red-edge
309 (Nov.)	*E. elaeagnus*	Chlorophyll Stress Other	Chlorophyll Red-edge
	R. davurica	Chlorophyll LAI Stress	Chlorophyll Red-edge Stress

All of the patterns observed from this analysis are imperfect. They are useful for understanding possible relationships between these species and certain vegetation indices, but I would advise caution when attempting to extrapolate these patterns to autumn olive or buckthorn in general, or about the entirety of the year instead of these four specific times. It is challenging to detect patterns, and I would not advise further dimensionality reduction without further research. It may be tempting and computationally easier to conduct an analysis based on only one type of vegetation index (for example, only using stress-related indices to analyze autumn olive), but I do not believe the patterns noted in this study are strong enough to justify that approach. I would advise almost the opposite – ruling out vegetation indices to use instead of narrowing down to one type; for example, it may not be very useful to use stress indices to analyze buckthorn, and it might be safe to ignore LAI indices for olive in the later part of the year. However, chlorophyll-related indices are so universal they cannot be discounted, and I would not feel confident about narrowing the filter more without further study.

Vegetation index patterns present in Figure 4, comparing the species of interest to themselves across the four months, appear most obviously in component 2. Several vegetation indices show up in the same place for both autumn olive and buckthorn, including MCARI and MCARI/OSAVI in the negative direction of component 2. For both species, this direction in component 2 is associated with the data from April and June, the earlier months of this analysis, and both these indices are associated with chlorophyll content and levels of nitrogen in the leaves. It makes sense that chlorophyll-focused VIs would separate the early months from the later months, when leaves are beginning to senesce. Furthermore, Carter2, which appears in the negative direction of component 1 for both species, and is therefore associated with the data from November and April, is an index related to stress. It also makes sense that the very beginning and end of the growing season would be periods where the plant is experiencing abnormal levels of stress, and this is measurable in that index for both species.

Finally, it is of note that in many cases, component 2 explains more variance than component 1. This is abnormal in PLS-DAs in general, and is particularly pronounced in the data for autumn olive. It is further surprising that, even when component 2 explains more variance, the data separates more distinctly in the component 1 direction shows less overlap in that component, almost uniformly across all months and both species. This phenomenon does not change the validity of the data, but the abnormality should be noted.

4.3 *Separating Species by Growing Season*

I will now shift my attention from vegetation indices to the data separation visible in Figures 2 – 4, and the second research question of this paper: "When in the growing season are spectra within each species most differentiable using vegetation indices?" As discussed in section 3.1, autumn olive separates out best from the rest of the field in June. This, in combination with the information from Table 3 regarding autumn olive in June, tells us that this separation is likely detectable via vegetation indices through some difference in the chlorophyll content of autumn olive plants, and to a lesser extent LAI, with some influence from stress-related indices. However, as discussed in section 3.3, autumn olive separates out very poorly from itself across the four times in the year. This would suggest that its leaves do not change very much in terms of chlorophyll content and stress levels, and LAI throughout the year, and that the features that distinguish it from other plants in June should be similarly helpful in distinguishing it in other months. Indeed, as discussed in section 3.1 this plant separates reasonably from the rest of the field in all months, although it is most noticeable in June. This also aligns with the life cycle of the plant – it grows its leaves in April, and maintains them until late in the fall, sometimes deep into winter (Warne, 2018). It is a hardy plant that outcompetes most native species. These factors contribute to a relative lack of change in phenotypes of this plant throughout the year, and explain the poor separation of this species in Fig. 3.

Buckthorn does not separate as well from the field. Its strongest months for this are June and November, and to a lesser extent September, as seen in Figure 3. Figure 4 supports this information, with the best separation happening in the later months, and to a lesser extent June, but relatively poor separation in April. In November, buckthorn is most effectively differentiated (in component 2) by vegetation indices related to LAI and stress, and is only positively associated with those types of indices (Table 3). This is one of the very few instances in which VIs related to chlorophyll do not play an important role. This causes the separation in Figure 3 to be most pronounced in November, and for that month to be one of the strongest separators in Figure 4 for this species. As this is the latest month in the year from which I have data, it would make sense for this to be the case, if buckthorn leaves did not senesce for a long time. Chlorophyll content that differs from the field would indicate that the plants leaves were a different color, but LAI and stress in November may be more indicative of a plant that still has leaves when most of its neighbors are bare. Indeed, this is exactly what sources tell us (Minnesota Department of Agriculture, 2013). Buckthorn can be easily spotted in the late fall/early winter, because they retain their leaves longer than most native species, giving them a competitive edge and contributing to their status as invasive.

4.4 *Areas for future research*

The findings of this study constitute only a fraction of results achievable through this method of inquiry. Using vegetation indices to filter hyperspectral data in order to detect and identify invasive plants is applicable to a wide variety of locations, landscapes, and species (Asner & Martin, 2008; Chance et al., 2016). Even in the testing area used for this research, only two invasive species were investigated, while at least double that amount existed in the same field, and likely several more in nearby fields. The first and most obvious direction in which to study further is simply to increase the range of the project, whether that be in the plant(s) of interest, location, climate, or a combination of these.

There are also several ways in which the research presented here could have been more thorough. I looked at one field on four days throughout the year. This is not a very large sample size from which to draw conclusions, and although I feel confident my results are applicable to this field at these times of year, I would be cautious about extrapolating them to other locations or times. If environmental conditions were inconsistent across the data collection timeframe, it could introduce additional uncertainty to the analysis – different reflectance values may be recorded on sunny days and cloudy days, and particularly windy days may alter LAI and leaf distribution. Before generalizing my results to other locations, I would prefer to conduct further analysis with slightly less time between data sets, perhaps once per month, and with consistent environmental conditions across collection dates. A slightly higher temporal resolution may be useful in more thoroughly answering my second guiding research question – when is the best time to differentiate these species?

For the third research question, aimed at exploring which biochemical and phenotypic characteristics were driving the differentiation in spectral signatures, it would be useful to have a source of independent verification. For example, certain vegetation indices are said to estimate stress levels of a plant, but a vegetation index is only reflectance data from different bands of light. If plant stress were directly measured, and those data supported the findings of this study, it would increase the confidence in vegetation index-derived results. I would be able to say with more surety that increased stress leads to a certain plant differentiating itself from the rest of the field via a certain vegetation index.

CONCLUSION

In summary, I was able to filter hyperspectral data through the lens of vegetation indices, and use a PLS-DA to individually differentiate two species of interest, autumn olive and Dahurian buckthorn, from the rest of the field at four times in the growing season. The species of interest did not always differentiate strongly from the rest of the field, but each species had at least one month of significant separation, and overall, June and November were the most useful months for differentiating these species. I further was able to analyze which vegetation indices were most useful for separating these species, and investigate patterns in the plant characteristics measured by these indices. Although they were not very strong, patterns nevertheless emerged, and in particular, the indices R0, MPRI, and SR5 showed a strong association with differentiating autumn olive in component 1. I also investigated the variance within each species of interest across the four months, and found that autumn olive is very consistent with itself, only differentiating slightly in June, but buckthorn separates from itself relatively well across time, with the data from late in the growing season being the most distinct. I believe this research helps establish a groundwork upon which a method for automatic detection and classification of invasive species from hyperspectral drone imagery can be built.

REFERENCES

Aneece, I., & Epstein, H. (2015). Distinguishing Early Successional Plant Communities Using Ground-Level Hyperspectral Data. *Remote Sensing*, *7*, 16588–16606. https://doi.org/10.3390/rs71215850

Asner, G. P., & Martin, R. E. (2008). Spectral and chemical analysis of tropical forests: Scaling from leaf to canopy levels. *Remote Sensing of Environment*, *112*(10), 3958–3970. https://doi.org/10.1016/j.rse.2008.07.003

Asner, G. P., & Vitousek, P. M. (2005). Remote analysis of biological invasion and biogeochemical change. *Proceedings of the National Academy of Sciences of the United States of America*, *102*(12), 4383–4386. https://doi.org/10.1073/pnas.0500823102

Barker, M., & Rayens, W. (2003). Partial least squares for discrimination. *Journal of Chemometrics*, *17*(3), 166–173. https://doi.org/10.1002/cem.785

Blackburn, G. A. (2007). Hyperspectral remote sensing of plant pigments. *Journal of Experimental Botany*, *58*(4), 855–867. https://doi.org/10.1093/jxb/erl123

Bowers, M. A. (1997). *University of Virginia's Blandy Experimental Farm*. https://doi.org/10.2307/20168167

Castro, K. L., Sánchez-Azofeifa, G. A., & Caelli, T. (2004). Discrimination of lianas and trees with leaf-level hyperspectral data. *Remote Sensing of Environment*, *90*(3), 353–372. https://doi.org/10.1016/j.rse.2004.01.013

Castro-Esau, K. L., Sánchez-Azofeifa, G. A., & Rivard, B. (2006). Comparison of spectral indices obtained using multiple spectroradiometers. *Remote Sensing of Environment*, *103*(3), 276–288. https://doi.org/10.1016/j.rse.2005.01.019

Chance, C. M., Coops, N. C., Plowright, A. A., Tooke, T. R., Christen, A., & Aven, N. (2016). Invasive Shrub Mapping in an Urban Environment from Hyperspectral and LiDAR-Derived Attributes. *Frontiers in Plant Science*, *7*, 1528. https://doi.org/10.3389/fpls.2016.01528

Clark, M. L., Roberts, D. A., & Clark, D. B. (2005). Hyperspectral discrimination of tropical rain forest tree species at leaf to crown scales. *Remote Sensing of Environment*, *96*(3), 375–398. https://doi.org/10.1016/j.rse.2005.03.009

Cochrane, M. (2000). Using vegetation reflectance variability for species level classification of hyperspectral data. *International Journal of Remote Sensing - INT J REMOTE SENS*, *21*, 2075–2087. https://doi.org/10.1080/01431160050021303

Dechant, B., Cuntz, M., Vohland, M., Schulz, E., & Doktor, D. (2017). Estimation of photosynthesis traits from leaf reflectance spectra: Correlation to nitrogen content as the dominant mechanism. *Remote Sensing of Environment*, *196*, 279–292. https://doi.org/10.1016/j.rse.2017.05.019

Gaertner, M., Den Breeyen, A., Hui, C., & Richardson, D. M. (2009). Impacts of alien plant invasions on species richness in Mediterranean-type ecosystems: A meta-analysis. *Progress in Physical Geography: Earth and Environment*, *33*(3), 319–338. https://doi.org/10.1177/0309133309341607

Große-Stoltenberg, A., Hellmann, C., Thiele, J., Werner, C., & Oldeland, J. (2018). Early detection of GPP-related regime shifts after plant invasion by integrating imaging spectroscopy with airborne LiDAR. *Remote Sensing of Environment*, *209*, 780–792. https://doi.org/10.1016/j.rse.2018.02.038

Gurevitch, J., & Padilla, D. (2004). Are invasive species a major cause of extinctions? *Trends in Ecology & Evolution*, *19*(9), 470–474. https://doi.org/10.1016/j.tree.2004.07.005

Heneghan, L., Fatemi, F., Umek, L., Grady, K., Fagen, K., & Workman, M. (2006). The invasive shrub European buckthorn (Rhamnus cathartica, L.) alters soil properties in Midwestern U.S. woodlands. *Applied Soil Ecology*, *32*(1), 142–148. https://doi.org/10.1016/j.apsoil.2005.03.009

Hochberg, E. J., Roberts, D. A., Dennison, P. E., & Hulley, G. C. (2015). Special issue on the Hyperspectral Infrared Imager (HyspIRI): Emerging science in terrestrial and aquatic ecology, radiation balance and hazards. *Remote Sensing of Environment*, *167*, 1–5. https://doi.org/10.1016/j.rse.2015.06.011

Huang, C., & Asner, G. P. (2009). Applications of Remote Sensing to Alien Invasive Plant Studies. *Sensors*, *9*(6), 4869–4889. https://doi.org/10.3390/s90604869

Kaufmann, H., Segl, K., Guanter, L., Hofer, S., Foerster, K.-P., Stuffler, T., Mueller, A., Richter, R., Bach, H., Hostert, P., & Chlebek, C. (2008). Environmental Mapping and Analysis Program (EnMAP)—Recent Advances and Status. *IGARSS 2008 - 2008 IEEE International Geoscience and Remote Sensing Symposium*, *4*, IV-109-IV–112. https://doi.org/10.1109/IGARSS.2008.4779668

Kganyago, M., Odindi, J., Adjorlolo, C., & Mhangara, P. (2017). Selecting a subset of spectral bands for mapping invasive alien plants: A case of discriminating Parthenium hysterophorus using field spectroscopy data. *International Journal of Remote Sensing*, *38*(20), 5608–5625. https://doi.org/10.1080/01431161.2017.1343510

Kimothi, M., & Dasari, A. (2010). Methodology to map the spread of an invasive plant (Lantana camara L.) in forest ecosystems using Indian remote sensing satellite data. *International Journal of Remote Sensing*, *31*, 3273–3289. https://doi.org/10.1080/01431160903121126

Knight, K. S., Kurylo, J. S., Endress, A. G., Stewart, J. R., & Reich, P. B. (2007). Ecology and ecosystem impacts of common buckthorn (Rhamnus cathartica): A review. *Biological Invasions*, *9*(8), 925–937. https://doi.org/10.1007/s10530-007-9091-3

Lehnert, L. W., Meyer, H., Meyer, N., Reudenbach, C., & Bendix, J. (2014). A hyperspectral indicator system for rangeland degradation on the Tibetan Plateau: A case study towards spaceborne monitoring. *Ecological Indicators*, *39*, 54–64. https://doi.org/10.1016/j.ecolind.2013.12.005

Lehnert, L. W., Meyer, H., Obermeier, W. A., Silva, B., Regeling, B., & Bendix, J. (2019). Hyperspectral Data Analysis in R: The hsdar Package. *Journal of Statistical Software*, *89*, 1–23. https://doi.org/10.18637/jss.v089.i12

Mahlein, A.-K., Steiner, U., Dehne, H.-W., & Oerke, E.-C. (2010). Spectral signatures of sugar beet leaves for the detection and differentiation of diseases. *Precision Agriculture*, *11*(4), 413–431. https://doi.org/10.1007/s11119-010-9180-7

Malinich, E., Lynn-Bell, N., & Kourtev, P. S. (2017). The effect of the invasive Elaeagnus umbellata on soil microbial communities depends on proximity of soils to plants. *Ecosphere*, *8*(5), e01827. https://doi.org/10.1002/ecs2.1827

Martin, M. E., & Aber, J. D. (1997). High Spectral Resolution Remote Sensing of Forest Canopy Lignin, Nitrogen, and Ecosystem Processes. *Ecological Applications*, *7*(2), 431–443. https://doi.org/10.1890/1051-0761(1997)007[0431:HSRRSO]2.0.CO;2

Mascaro, J., & Schnitzer, S. A. (2007). Rhamnus cathartica L. (Common Buckthorn) as an Ecosystem Dominant in Southern Wisconsin Forests. *Northeastern Naturalist*, *14*(3), 387–402.

Matongera, T., Mutanga, O., & Lottering, R. (2016). Detection and mapping of bracken fern weeds using multispectral remotely sensed data: A review of progress and challenges. *Geocarto International*. https://doi.org/10.1080/10106049.2016.1240719

Meyer, H., Lehnert, L. W., Wang, Y., Reudenbach, C., Nauss, T., & Bendix, J. (2017). From local spectral measurements to maps of vegetation cover and biomass on the Qinghai-Tibet-Plateau: Do we need hyperspectral information? *International Journal of Applied Earth Observation and Geoinformation*, *55*, 21–31. https://doi.org/10.1016/j.jag.2016.10.001

Minnesota Department of Agriculture. *Buckthorn: What You Should Know. What You Can Do.*, State of Minnesota, Saint Paul, MN, 2013

Mutanga, O., Skidmore, A. K., & Prins, H. H. T. (2004). Predicting in situ pasture quality in the Kruger National Park, South Africa, using continuum-removed absorption features. *Remote Sensing of Environment*, *89*(3), 393–408. https://doi.org/10.1016/j.rse.2003.11.001

Naumann, J. C., Bissett, S. N., Young, D. R., Edwards, J., & Anderson, J. E. (2010). Diurnal patterns of photosynthesis, chlorophyll fluorescence, and PRI to evaluate water stress in the invasive species, Elaeagnus umbellata Thunb. *Trees*, *24*(2), 237–245. https://doi.org/10.1007/s00468-009-0394-0

Oliphant, A. J., Wynne, R. H., Zipper, C. E., Ford, W. M., Donovan, P. F., & Li, J. (2017). Autumn olive (Elaeagnus umbellata) presence and proliferation on former surface coal mines in Eastern USA. *Biological Invasions*, *19*(1), 179–195. https://doi.org/10.1007/s10530-016-1271-6

Peerbhay, K., Mutanga, O., & Ismail, R. (2016). The identification and remote detection of alien invasive plants in commercial forests: An Overview. *South African Journal of Geomatics*, *5*(1), 49–67. https://doi.org/10.4314/sajg.v5i1.4

Royimani, L., Mutanga, O., Odindi, J., Dube, T., & Matongera, T. N. (2019). Advancements in satellite remote sensing for mapping and monitoring of alien invasive plant species (AIPs). *Physics and Chemistry of the Earth, Parts A/B/C*, *112*, 237–245. https://doi.org/10.1016/j.pce.2018.12.004

Sanchez-Azofeifa, G. A., Calvo-Alvarado, J., Espírito-Santo, M., Fernandes, G., Powers, J., & Quesada, M. (2013). *Tropical Dry Forests in the Americas: The Tropi-Dry Endeavor* (pp. 1–16).

Schmidt, K., & Skidmore, A. (2003). *Spectral discrimination of vegetation types in a coastal wetland*. https://doi.org/10.1016/S0034-4257(02)00196-7

Skowronek, S., Ewald, M., Isermann, M., Van De Kerchove, R., Lenoir, J., Aerts, R., Warrie, J., Hattab, T., Honnay, O., Schmidtlein, S., Rocchini, D., Somers, B., & Feilhauer, H. (2017). Mapping an invasive bryophyte species using hyperspectral remote sensing data. *Biological Invasions*, *19*(1), 239–254. https://doi.org/10.1007/s10530-016-1276-1

Thenkabail, P., Gumma, M. K., Pardhasaradhi Teluguntla, & Mohammed Irshad Ahmed. (2014). Hyperspectral Remote Sensing of Vegetation and Agricultural Crops. *Photogrammetric Engineering & Remote Sensing (PE&RS);80,(2014) Pagination 697,723*. https://repo.mel.cgiar.org/handle/20.500.11766/5374

Underwood, E. C., Ustin, S. L., & Ramirez, C. M. (2007). A comparison of spatial and spectral image resolution for mapping invasive plants in coastal california. *Environmental Management*, *39*(1), 63–83. https://doi.org/10.1007/s00267-005-0228-9

Ustin, S. L., & Jacquemoud, S. (2020). How the Optical Properties of Leaves Modify the Absorption and Scattering of Energy and Enhance Leaf Functionality. In J. Cavender-Bares, J. A. Gamon, & P. A. Townsend (Eds.), *Remote Sensing of Plant Biodiversity* (pp. 349–384). Springer International Publishing. https://doi.org/10.1007/978-3-030-33157-3_14

Ustin, S. L., Roberts, D. A., Gamon, J. A., Asner, G. P., & Green, R. O. (2004). Using imaging spectroscopy to study ecosystem processes and properties. *BioScience*. https://scholar.google.com/scholar_lookup?title=Using+imaging+spectroscopy+to+study+ecosystem+processes+and+properties&author=Ustin%2C+S.L.&publication_year=2004

Wang, A., Zhang, W., & Wei, X. (2019). A review on weed detection using ground-based machine vision and image processing techniques. *Computers and Electronics in Agriculture*, *158*, 226–240. https://doi.org/10.1016/j.compag.2019.02.005

Warne, Amanda. 2018. Autumn olive (Elaeagnus umbellata) Best Management Practices in Ontario. Ontario Invasive Plant Council, Peterborough, ON.

Wilfong, B. N., Gorchov, D. L., & Henry, M. C. (2009). Detecting an Invasive Shrub in Deciduous Forest Understories Using Remote Sensing. *Weed Science*, *57*(5), 512–520. https://doi.org/10.1614/WS-09-012.1

Xiao, Y., Zhao, W., Zhou, D., & Gong, H. (2014). Sensitivity Analysis of Vegetation Reflectance to Biochemical and Biophysical Variables at Leaf, Canopy, and Regional Scales. *IEEE Transactions on Geoscience and Remote Sensing*, *52*(7), 4014–4024. https://doi.org/10.1109/TGRS.2013.2278838

Yang, M.-D., Huang, K.-S., Yang, Y. F., Lu, L.-Y., Feng, Z.-Y., & Tsai, H. P. (2016). Hyperspectral Image Classification Using Fast and Adaptive Bidimensional Empirical Mode Decomposition With Minimum Noise Fraction. *IEEE Geoscience and Remote Sensing Letters*, *13*(12), 1950–1954. https://doi.org/10.1109/LGRS.2016.2618930